

---

# More Than Meets the Eye: Self-Supervised Depth Reconstruction From Brain Activity

---

Guy Gaziv

Michal Irani

Dept. of Computer Science and Applied Math  
The Weizmann Institute of Science

## Abstract

In the past few years, significant advancements were made in reconstruction of observed natural images from fMRI brain recordings using deep-learning tools. Here, for the first time, we show that dense 3D depth maps of observed 2D natural images can also be recovered directly from fMRI brain recordings. We use an off-the-shelf method to estimate the unknown depth maps of natural images. This is applied to both: (i) the small number of images presented to subjects in an fMRI scanner (images for which we have fMRI recordings – referred to as “paired” data), and (ii) a very large number of natural images with no fMRI recordings (“unpaired data”). The estimated depth maps are then used as an auxiliary reconstruction criterion to train for depth reconstruction directly from fMRI. We propose two main approaches: Depth-only recovery and joint image-depth RGBD recovery. Because the number of available “paired” training data (images with fMRI) is small, we enrich the training data via self-supervised cycle-consistent training on many “unpaired” data (natural images & depth maps without fMRI). This is achieved using our newly defined and trained Depth-based Perceptual Similarity metric as a reconstruction criterion. We show that predicting the depth map *directly from fMRI* outperforms its indirect sequential recovery from the reconstructed images. We further show that activations from early cortical visual areas dominate our depth reconstruction results, and propose means to characterize fMRI voxels by their degree of depth-information tuning. This work adds an important layer of decoded information, extending the current envelope of visual brain decoding capabilities.

Code: <https://github.com/WeizmannVision/SelfSuperReconst>

## 1 Introduction

Decoding observed visual scene information from brain activity may form the basis for brain-machine interfaces and for understanding visual processing in the brain (Fig 1). A classic challenge in this domain is reconstructing seen natural images from their recorded fMRI<sup>1</sup> brain activity [1–4]. To learn such mappings, fMRI datasets provide pairs of images and their corresponding fMRI responses, referred to here as “paired” data. The goal in that challenge is to learn fMRI-to-image decoding which generalizes well to image reconstruction from novel “test-fMRIs” induced by novel images.

However visual scene understanding goes well beyond the RGB bitmap which represents it. An important complementary cue to natural-image understanding is inferring depth relations within it [5]. Humans perform well on monocular depth estimation by exploiting cues such as perspective, scaling relative to the known size of familiar objects, shading and occlusion [6]. Furthermore, previous studies found evidence for depth cue encoding and integration in the human visual cortex [7, 8].

In this paper propose a new challenge, which goes beyond the traditional fMRI-to-image reconstruction task: ***Given an fMRI recording of an observed scene (a 2D image), reconstruct its underlying***

<sup>1</sup>functional magnetic resonance imaging.

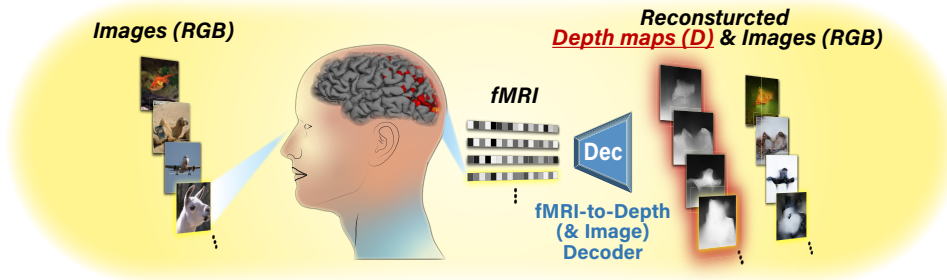


Figure 1: **The task: reconstructing dense depth maps (D) from fMRI brain recordings.**

**dense 3D depth map (D) directly from fMRI.** This can be done in addition to (or without) recovering the observed RGB image. Adding this additional layer of depth information to the fMRI decoding problem has two potential implications: (i) It paves the way to reconstructing *new types of inferred dense information about a scene that is not explicitly presented to the subject*, and (ii) it provides auxiliary criteria to guide and train image-reconstruction networks, which complements existing reconstruction criteria based purely on RGB data.

**Prior work on image reconstruction from fMRI.** fMRI-to-Image reconstruction methods can broadly be classified into three main categories: (i) Linear regression between fMRI data and handcrafted image-features (e.g., Gabor wavelets) [9, 4, 10], (ii) Linear regression between fMRI data and pre-trained deep image-features – e.g., features of pretrained AlexNet [11–14], or latent spaces of pretrained generative models [15–18], and (iii) End-to-end Deep Learning [19–24].

Most of these methods inherently rely on “paired” data to train their decoder (pairs of images and their corresponding fMRI responses). In the typical case, when only a small number of such pairs are available, purely supervised models are prone to overfitting. This leads to poor generalization to new test-data (fMRI response evoked by new images). Recently, [23, 24] proposed to cope with the limited “paired” training examples by adding self-supervision on additional “unpaired” natural images (images with no fMRI recording). This led to state-of-the-art results in image-reconstruction. However, all the above methods focused on reconstructing only images and semantic features, glossing over other important visual perception cues, such as scene depth. This is the focus of the current paper.

We present a new approach that generalizes the self-supervised approach of [23, 24] to accommodate for *recovery of dense depth maps directly from fMRI*. Our approach is illustrated in Fig 2:

- We first estimate the depth maps of natural images using an off-the-shelf pretrained network (“MiDaS” [25]) for monocular depth estimation (Fig 2a). This is applied both to the scarce “paired” images in the fMRI dataset, as well as to many more “unpaired” natural images from ImageNet. This step provides us with surrogate “ground-truth” Depth information, which can either be used on its own for training our network, or can be combined with the source image to provide new RGBD “ground-truth” data for training.
- We then train two types of deep networks: (i) an Encoder *Enc*, that encodes depth-based information (either Depth alone, or RGBD data) into their corresponding fMRI responses (Fig 2c), and (ii) a Decoder *Dec*, that decodes fMRI recordings to their corresponding depth-based information (Fig 2d1). Concatenating those two networks back-to-back, *Enc-Dec*, yields a combined network whose input and output are the same depth-based information (Fig. 2c2). **This allows for unsupervised training on unpaired data** (i.e., Depth maps or RGBD data *without fMRI recordings*, e.g., obtained from 50,000 randomly sampled natural images from ImageNet in our experiments). Such self-supervision adapts the network to the statistics of never-before-seen depth-based data.
- The loss enforced on the reconstructed depth-based information employs a special **Depth-based Perceptual Similarity**, which we also present in this paper (Fig 2b). This encourages our reconstructed depth maps to be *perceptually meaningful*.

Fig 3 shows image & depth reconstructions using our RGBD-based approach. These results demonstrate a new capability of dense Depth recovery directly from fMRI (in addition to RGB image reconstruction). We show that training our networks on Depth-only data or on RGBD data provide comparable quality of depth-map reconstructions from fMRI (Fig 4bc). We further show that depth reconstructions *directly from fMRI* provide significantly better results than *indirect depth estimation* applied (after the fact) to purely reconstructed RGB-images. Lastly, training our networks on the combined RGBD data further allows us to explore whether there are fMRI voxels more tuned to depth information, versus voxels more tuned to RGB information. These experiments are discussed in Sec. 4.

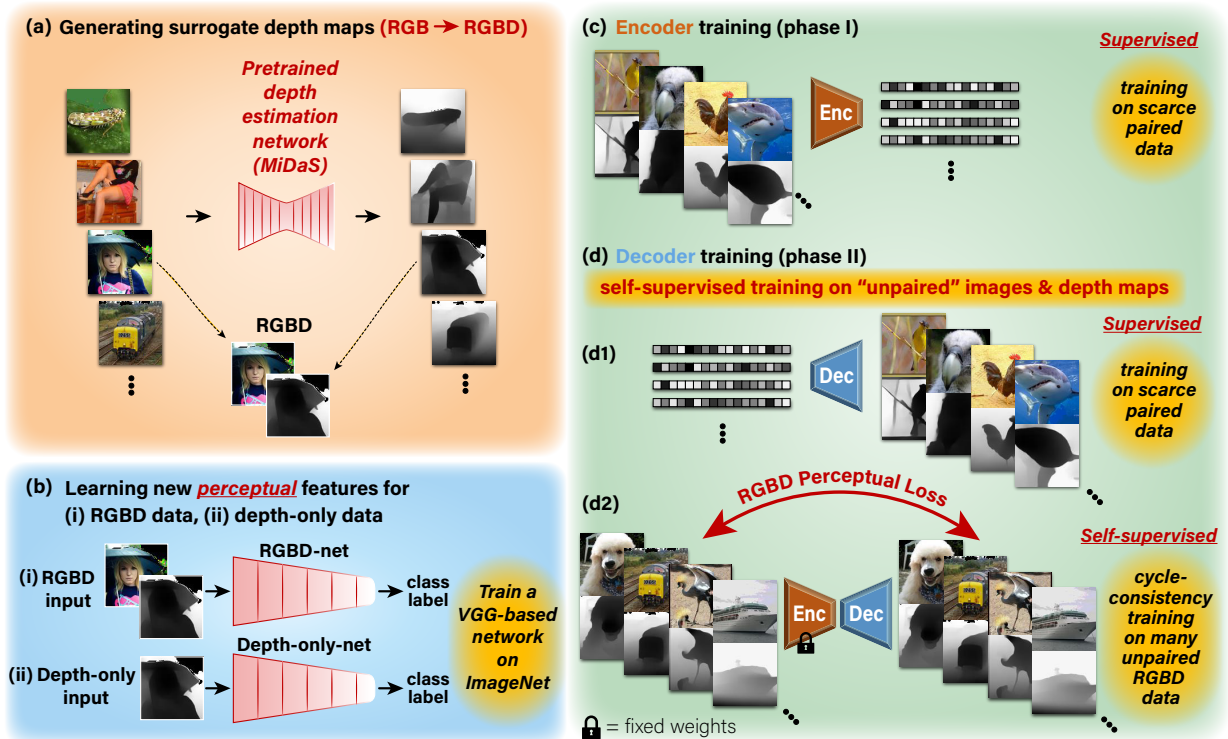


Figure 2: **Our proposed method.** (a) Predicting depth maps for all ground truth images (RGB) using a pretrained network (“MiDaS” [25]). This includes the images in the paired fMRI dataset and those in the external dataset of unpaired natural images. (b) Learning depth perceptual features. We train two VGG-based networks for ImageNet object recognition for either input type, RGBD or Depth-only. These networks give rise to new types of perceptual metrics for Decoder training and provide the Encoder backbone. (c) Phase I: Supervised training of the Encoder with “paired” training data. (d) Phase II: Training the Decoder with two types of data simultaneously: (d1) The “paired” training data (supervised examples), and (d2) “unpaired” natural images with their depth maps (self-supervision). The pretrained Encoder from phase I is kept fixed in phase II.

Our contributions are therefore several-fold:

- The first method to reconstruct dense 3D depth information from brain activity.
- A self-supervised approach for reconstructing depth-based information (*Depth-only* or *RGBD*) directly from fMRI recordings, despite having only scarce fMRI training data.
- A *Depth-based Perceptual Similarity* measure, based on specially trained *perceptual depth features*.
- Characterize brain-voxels by their degree of depth-sensitivity via a novel depth-sensitivity measure.

## 2 Overview of the approach

Our goal is to reconstruct dense depth 3D information from fMRI data of observed 2D color images. For that purpose we explored three main approaches: (i) Decoding depth-only information *directly from fMRI*; (ii) Simultaneous decoding of images+depth information (RGBD) *directly from fMRI*; (iii) *Indirect* depth reconstruction computed (after the fact) from RGB images which were reconstructed from fMRI. Our experimental results show (see Sec. 4) that reconstructing depth directly from fMRI (approaches (i) & (ii)) are significantly superior to sequential indirect depth reconstruction (approach (iii)). Fig 2 shows our proposed framework for direct depth reconstruction from fMRI. It consists of three main components:

**1. Generating surrogate depth data (Fig 2a).** Our training of a depth decoder requires the underlying ground-truth depth maps of natural images. To obtain these data we generate depth maps by feeding-forward the natural images through an off-the-shelf monocular depth estimation method for natural images, called MiDaS [25]. We then use these maps as our surrogate “ground-truth” depth data. We estimated the depth maps of all 1250 images of ‘fMRI on ImageNet’ [26], and all those of ImageNet classification challenge (ILSVRC) [27]. These depth-maps are then used in the following steps.

**2. Learning semantically-meaningful depth features for depth-based perceptual similarity (Fig 2b).** Our trained Decoder (fMRI  $\mapsto$  Depth, or fMRI  $\mapsto$  RGBD) requires a similarity score/loss on the

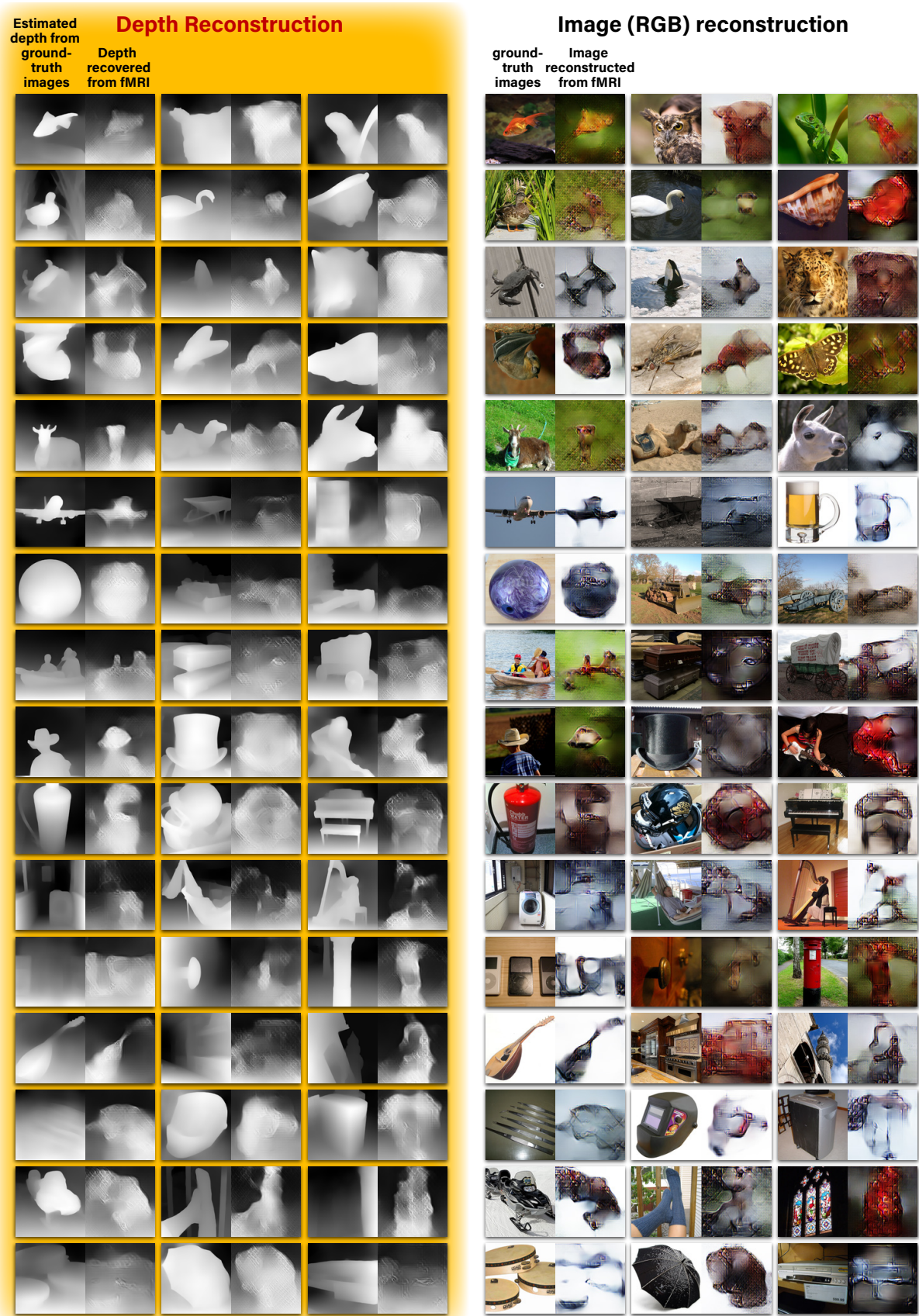


Figure 3: **Image & Depth (RGBD) reconstruction results.** (Left column): Depth maps reconstruction results side-by-side their estimated ground-truth from the original RGB images. (Right column): Image (RGB) reconstruction results side-by-side the ground-truth images presented to the human. We show results of test cohort of *fMRI on ImageNet* [26].

reconstructed depth maps. Perceptual Similarity [28] has been shown to be a powerful metric for many image reconstruction tasks. However, that metric was developed for images only. We propose here a new perceptually/semantically meaningful similarity score for depth maps. This is obtained by training from scratch two VGG-like networks, trained on ImageNet for the task of object recognition, but from depth-based inputs: (i) An RGBD network that receives a 4-channel RGBD input (an image concatenated channel-wise with its estimated depth map), and (ii) A Depth-only network that is trained similarly and with the same architecture, but with a single-channel input containing only the depth map of an image. The goal of such training is not to improve object recognition, but rather to obtain a coarse-to-fine hierarchy of semantically-meaningful depth-related features (depth-only features, or RGBD features). Once trained, these features form the basis to our RGBD and Depth-only Perceptual Similarity metrics used for training and evaluating our reconstructions.

**3. Handling the insufficient fMRI training data (Fig 2cd).** To train our Decoder (fMRI  $\mapsto$  Depth, or fMRI  $\mapsto$  RGBD), we used a moderate-size fMRI dataset – ‘fMRI on ImageNet’ [26]. However, the train-set of this dataset contains only 1200 pairs of images with their corresponding fMRI recordings (this small number is typical of fMRI datasets). Such a small number of examples cannot span the huge space of natural images (nor their corresponding depth maps), resulting in a poor generalization of the Decoder to fMRIs of never-before-seen images. To overcome this problem, we generalize the self-supervised approach of [23] to accommodate for depth information. This allows us to train our decoder on many (50,000) additional natural images with their estimated depth maps – images for which there are *no fMRI recordings*. Specifically, our semi-supervised approach employs a two-phase training: The first phase is supervised, and focuses on training of an Encoder, *Enc* – to map images and their depth maps to their corresponding fMRI recordings. This is done using the 1200 “paired” examples from the fMRI dataset, along with their MiDaS-estimated depth maps (Fig 2c). In the second phase, we train the Decoder, *Dec*, using two objectives: (i) supervised training, to map the limited “paired” fMRI recordings to their corresponding images and depth maps (Fig 2d1), and (ii) *self-supervised cycle-consistent training* on a very large number of “unpaired” natural images with their corresponding depth maps. This cycle-consistency is facilitated using the auxiliary pretrained Encoder from the first phase (Fig 2d2). The Decoder loss uses our above-mentioned *depth-based Perceptual Similarity* between the reconstructed and the “ground-truth” depth maps. Using this metric ensures that the reconstructed images and their reconstructed depth maps are perceptually and semantically meaningful (well beyond their pixel-level similarity).

We experimented with 2 main approaches to explore the best scheme for depth-decoding from fMRI:

**Depth-only framework.** Our goal is to recover depth. In this mode, the input to the Encoder & output of the Decoder (Fig 2cd) is a single-channel depth map; all RGB image data is discarded in the training. The reconstruction loss on the decoder in this case is our Depth-only Perceptual Similarity. This approach allowed us to isolate the task of depth recovery from fMRI alone. However, it risks poor Encoder-training in the first supervised phase. The reason being: there are likely many voxels in the visual cortex that are *not* depth-dependent, only RGB-dependent. Yet, the encoder is expected to predict their values from depth-only information in the first training phase.

**RGBD framework.** To avoid the above potential problem, we experimented also with training both the Encoder & Decoder on combined RGB-D data. The reconstruction loss on the decoder in this case is our RGBD Perceptual Similarity. This combined reconstruction further allows us to explore whether there are fMRI voxels more tuned to depth, versus voxels more tuned to RGB information. These experiments are discussed in Sec. 4.

### 3 Method Details

**Learning perceptually-meaningful Depth-based features.** Part of the success of our method stems from using perceptually-meaningful Depth-based features. These features are used in two main ways within our method: (i) They form the basis for our *Depth-based Perceptual Similarity* metric (explained next); (ii) They form the main backbone of our Encoder (a detailed description of our networks architecture is found in the Supplementary-Material). These perceptually-meaningful depth-based features are learned as follows: We customized the VGG architecture to accommodate a four-channel RGBD input, and another version that respects a single Depth-only input. We then train these networks from scratch on ImageNet for the task of object recognition (Fig 2b), similar to the way the original VGG network was trained. To obtain the “ground-truth” depth data required for this training, we estimated the depth maps of all  $\sim 1.3$ M images in ImageNet classification

challenge (ILSVRC) [27] using MiDaS. We denote the trained two *depth-based object recognition networks* as  $\varphi_{RGBD}$  and  $\varphi_D$ . Notably, the resulting object recognition accuracy of  $\varphi_{RGBD}$  was comparable with its RGB-only baseline ( $\sim 70\%$  accuracy), whereas the depth-only recognition network  $\varphi_D$  achieved  $\sim 42\%$  accuracy. The goal, however, was not to improve object recognition, but rather to obtain a coarse-to-fine hierarchy of semantically-meaningful depth-related features.

**Depth-based Perceptual Similarity.** We extend the concept of Perceptual Similarity metric of [28] from images to depth-related data (Depth-only or RGBD). Specifically, to compare a reconstructed depth map  $\hat{s}$  to a target depth map  $s$ , we first feed both into the trained Depth-only recognition network,  $\varphi_D$ , and extract features from multiple blocks (from low to high layers, corresponding to lower-to-higher “semantic” levels). Similarly, when  $s$  and  $\hat{s}$  are RGBD data, we use the trained RGBD-based recognition network,  $\varphi_{RGBD}$ . For brevity we henceforth refer to both networks as  $\varphi$ . We denote the deep features extracted from an input  $s$  at the output of a particular block  $b$ , by  $\varphi^b(s)$ . The perceptual similarity between  $s$  and  $\hat{s}$ ,  $\mathcal{L}_{perceptual}(\hat{s}, s)$ , is then defined by cosine similarity between channel-normalized ground-truth and predicted features at each block output:

$$\mathcal{L}_{perceptual}(\hat{s}, s) \propto - \sum_{b=1}^5 \cos(\angle(\varphi^b(\hat{s}), \varphi^b(s))), \quad (1)$$

**Handling the insufficient fMRI training data - The self-supervised approach:**

Fig 2cd shows our two-phase self-supervised training. We describe the method for the case of RGBD encoding/decoding, and then briefly highlight the differences in the Depth-only configuration.

• **Encoder supervised training (Phase I, Fig 2c).** Let  $r$  be the ground truth fMRI, and  $\hat{r} = Enc(s)$  denote the encoded fMRI resulting from applying our Encoder to an RGBD input,  $s$ . We define an fMRI loss by a convex combination of mean square error and cosine proximity between  $\hat{r}$  and  $r$ :

$$\mathcal{L}_r(\hat{r}, r) = \alpha \cdot \text{MSE}(\hat{r}, r) - (1 - \alpha) \cos(\angle(\hat{r}, r)), \quad (2)$$

where  $\alpha$  is a hyperparameter set empirically ( $\alpha = 0.9$ ). We use this loss for training the Encoder  $E$ . Upon completion of Encoder training, we proceed to training the Decoder with a fixed Encoder.

• **Decoder training (Phase II, Fig 2d).** Decoder training is driven by two main losses:

$$\mathcal{L}^{Dec} + \mathcal{L}^{EncDec}, \quad (3)$$

where  $\mathcal{L}^{Dec}$  is a supervised loss on training pairs of image-fMRI, and  $\mathcal{L}^{EncDec}$  (Encoder-Decoder) is an *unsupervised* loss on unpaired images (without corresponding fMRI recordings). Both components of the loss are normalized to have the same order of magnitude (all in the range  $[0, 1]$ , with equal weights), to guarantee that the total loss is not dominated by any individual component. We found our reconstruction results to be relatively insensitive to the exact balancing between the two-loss components. We next detail each component of the loss.

$\mathcal{L}^{Dec}$ : *Decoder Supervised Training* (Fig 2d1). Given training pairs  $\{(r, s)\} = \{\text{fMRI, RGBD}\}$ , the supervised loss  $\mathcal{L}^{Dec}$  is imposed on the decoded RGBD image,  $\hat{s} = Dec(r)$ .  $\mathcal{L}^{Dec} = \mathcal{L}_s(\hat{s}, s)$  consists of an  $\ell_1$ -loss on the RGBD values, as well as our depth-based perceptual loss,  $\mathcal{L}_{perceptual}$  (Eq. 1):

$$\mathcal{L}_s(\hat{s}, s) = \|\hat{s} - s\|_1 + \mathcal{L}_{perceptual}(\hat{s}, s) + \mathcal{R}(\hat{s}) \quad (4)$$

where,  $\mathcal{R}(\hat{s})$ , corresponds to total variation (TV) regularization of the reconstructed (decoded)  $\hat{s}$ .

$\mathcal{L}^{ED}$ : **Self-supervised Encoder-Decoder training on unpaired Natural Images & Depth Maps** (Fig 2d2). This objective enables to train on any desired unpaired image along with its corresponding depth map (images for which fMRI was never recorded), well beyond the 1200 images included in the fMRI dataset. In particular, we used  $\sim 50K$  additional natural images from ImageNet’s 1000-class data [27], along with their estimated depth-maps (see Sec. 2). We train on such RGBD data without fMRI, by imposing cycle consistency through our Encoder-Decoder transformation:

$$s \mapsto \hat{s}_{EncDec} = D(E(s)).$$

The unsupervised component  $\mathcal{L}^{EncDec}$  of the loss in Eq. 3 on unpaired images,  $s$ , reads:

$$\mathcal{L}^{EncDec} = \mathcal{L}_s(\hat{s}_{EncDec}, s),$$

where  $\mathcal{L}_s$  is the Image loss defined in Eq. 4. In other words,  $\mathcal{L}^{EncDec}$  imposes cycle-consistency on any RGBD data, but at a perceptual level (not only at the pixel level).

The input to our Encoder (and output of our Decoder) are  $112 \times 112$  images and depth maps, although our method works well also on other resolutions. For details on hyperparameters as well as on Encoder/Decoder architectures see Supplementary-Material.

**Depth-only framework.** In a Depth-only configuration we encode/decode (reconstruct) the depth map alone, discarding all RGB data from training. Specifically, we switch to a Depth-only perceptual loss using  $\varphi_D^b$ . The Encoder/Decoder switch to a single channel input/output, respectively. Particularly, the Encoder architecture switches to using a Depth-only pretrained network.

**Runtime.** Our system completes the two-stage training within approximately 2 hours on a single Tesla V100 GPU. Inference (decoding of new fMRI recordings) takes a few milliseconds per image.

## 4 Experiments and Results

### 4.1 Experimental datasets

We tested our self-supervised depth reconstruction approach on a highly popular and publicly available benchmark fMRI dataset, called **fMRI on ImageNet** [26]. We found this dataset to be the only one currently suitable for our method in terms of the stimuli used and fMRI signal quality. An important point is the requirement to perform depth estimation on color ImageNet-like natural images that match the input distribution expected by the MiDaS depth estimation network we used.

‘fMRI on ImageNet’ provides fMRI recordings of observed images. Subjects were instructed to fixate on a cross positioned at the center of the presented images. ‘fMRI on ImageNet’ comprises 1250 distinct ImageNet images drawn from 200 selected categories. Fifty image categories provided the 50 test images, one from each category. The remaining 1200 were defined as train set. The images in the train set and test set come from mutually exclusive categories (different classes). We considered approximately 4500 voxels from the visual cortex, provided by the authors of [26].

We used additional  $\sim 50K$  “unpaired” natural images from ImageNet’s validation set [27] *with their estimated depth maps*, for our self-supervised training (Fig. 2d2). We verified that the images in our additional unlabeled external dataset, are distinct from those in the ‘fMRI on ImageNet’.

### 4.2 Depth recovery - results & evaluations

Fig. 3 shows visual results of our proposed self-supervised RGBD method. This includes the reconstructed RGB images (of the underlying images seen by the subjects) and their corresponding reconstructed depth maps (never seen by the subjects) – both recovered directly from fMRI. A stark feature that emerges in the reconstructed depth maps is foreground/background segregation. However, a closer inspection reveals finer details of depth variations. Results are shown for the entire test cohort (all 50 test fMRIs of the ‘fMRI on ImageNet’ dataset). These results correspond to Subject 3, who has the highest noise-ceiling fMRI data (results on other subjects are in the Supplementary-Material).

**Performance evaluation.** To quantitatively evaluate our reconstruction results, we followed an  $n$ -way identification experiment [23, 24, 13, 16, 21, 14], applied separately to images (RGB) and to depth maps (D). Each reconstructed image is compared against  $n$  candidate images (the ground truth image, and  $(n - 1)$  other randomly selected images). The goal is to identify the ground truth, or at least rank it well among the candidates (rank=1 signifies perfect identification). We evaluate our RGB or Depth reconstructions using this rank identification (lower is better). This provides an informative accuracy measure that accounts for cases when the ground truth is not strictly identified as the best candidate, but is nevertheless ranked fairly low. Reconstructed *Images (RGB)* were compared against candidates using the image-based Perceptual Similarity metric of [28]. Reconstructed *depth maps* were compared against candidate depth maps using our new *Depth-only* Perceptual Similarity metric.

Fig 4 shows comparison of our three main approaches for depth recovery (see Sec 2). Specifically, it shows results for our two main approaches to depth-decoding from fMRI, which achieved the best results: (i) RGBD framework (Fig 4b), and (ii) Depth-only framework (training for depth recovery without any RGB data during training, Fig 4c). We find that both approaches successfully recover depth details as demonstrated in the visual results. Furthermore, quantitative rank identification evaluation scores a mean rank of 120 and 124 in the challenging 1000-way task for RGBD and Depth-only methods, respectively – more than 4x the chance level (chance level rank=500, showing average scores over all 5 subjects). Comparing these approaches, we find that the results by both approaches are largely on par with each other. This implies that best depth recovery results are

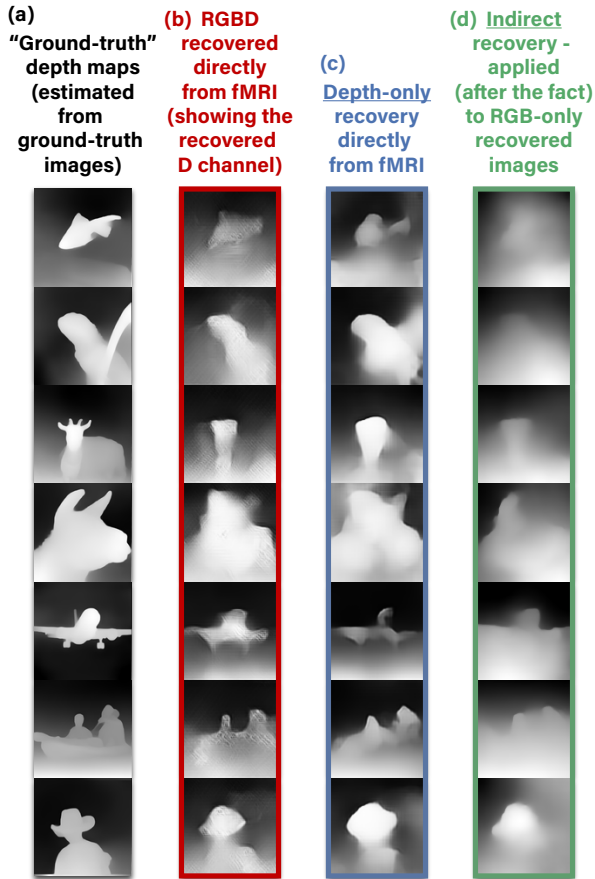


Figure 4: **Depth recovery by RGBD & Depth-only approaches.** (a) Depth map estimated from ground-truth RGB-image using MiDaS [25]. (b) Depth channel of RGBD reconstruction directly from fMRI. (c) Depth recovery directly from fMRI, where both Encoder & Decoder are trained “Depth-only” – without using any RGB data for training. (d) Indirect depth recovery from reconstructed RGB-images using MiDaS. This approach fails to recover depth faithfully. (e) Depth reconstruction mean rank for (b)-(d) respectively by  $n$ -way rank identification experiments (lower is better, showing average over all 50 reconstructed depth maps and five subjects). 95% Confidence Intervals by bootstrap shown on charts.

obtainable even in *complete absence of any RGB supervision or self-supervision*. On the other hand, the RGBD approach provides additional recovered information – the reconstructed RGB image.

### 4.3 Ablation study – The importance of Direct vs. Indirect depth reconstruction from fMRI

We compare our reconstruction results against several baselines:

- **RGB-only Enc/Dec followed by depth estimation on the reconstructed images.** Fig 4d shows results for an *indirect* depth recovery approach. We estimate the depth map from a reconstructed RGB image as a post-processing step (The RGB image is reconstructed via an RGB-only framework with the perceptual features/similarity of [28]). This involves no training on depth data at all. This approach gives rise to poor depth reconstruction quality, indicated both visually and quantitatively in Fig 4.

- **RGB-only Enc/Dec, but *constrained* by a depth estimation loss on the reconstructed images.** We extended the *indirect* depth recovery of the RGB-only framework, by imposing a depth loss on the reconstructed RGB images *during* training. To impose depth reconstruction criteria on an RGB-only Decoder, we mounted atop it the pre-trained MiDaS depth estimation network [25],  $\mathcal{M}(\cdot)$ . Although the Decoder itself does not produce any depth map, combining the resulting MiDaS depth map with the decoder’s RGB output provides an RGBD output in total. We experimented with two types of losses: (i) the standard loss of the RGBD framework,  $\mathcal{L}_s$ , which includes also depth perceptual similarity  $\mathcal{L}_{perceptual}$  (Eq. 1), and (ii) a simple  $\ell_1$ -loss on the depth maps,  $\|\mathcal{M}(\hat{s}_{rgb}) - \mathcal{M}(s_{rgb})\|_1$ .

The y-axis in Fig 5a shows the mean *depth-rank* in the challenging *1000-way* identification task (lower is better; shown for Subject 3; see Supp-Material for all subjects). The direct RGBD approach scores mean *depth-rank* of 97 (5x better than chance level), significantly outperforming the indirect approaches, (i) & (ii), by a large margin (38 and 56 rank levels, respectively). The depth recovery performance achieved by the *perceptually-constrained* indirect approach is slightly better than the two other indirect approaches for depth recovery (but significantly worse than the direct ones).

- **The RGB-Depth reconstruction Trade-off.** Fig 5a further plots the mean *depth-rank* versus the mean *RGB-rank* in the challenging *1000-way* identification task, for all the direct & indirect



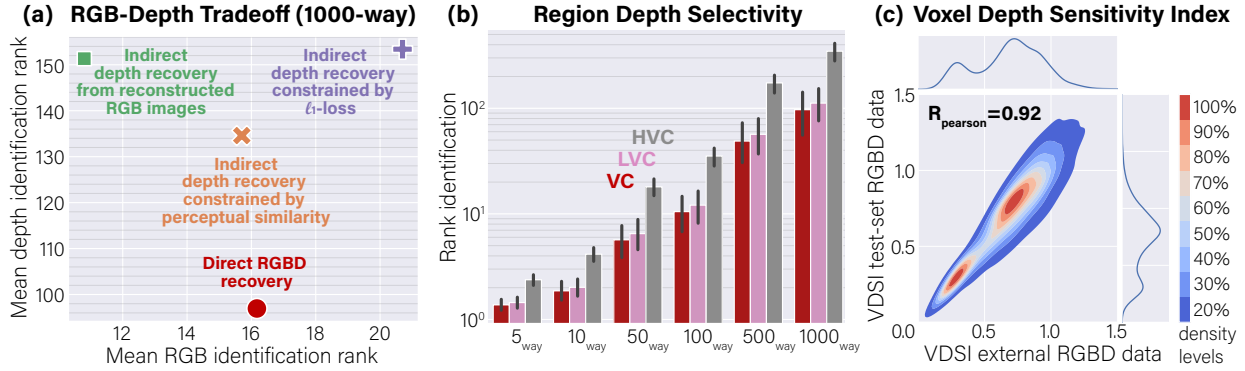


Figure 5: **Ablations study.** (See Sec 4.3 for details).

image+depth recovery approaches. Our results show that our direct RGBD approach provides the best depth reconstructions with yet a very good RGB identification score (a mean-RGB rank of 16 – more than 30x better than chance level). On the other hand, the RGB-only approach, which is trained solely for RGB recovery, gives rise to better (yet comparable) RGB reconstructions.

#### 4.4 Detecting depth-sensitive voxels

**Predominance of Lower Visual Cortex.** We analyzed the impact of using only a subset of voxels from particular brain regions. Fig 5b shows rank identification results when using only voxels from the Lower Visual Cortex (LVC, comprising V1-V3) or those from the Higher Visual Cortex (HVC, comprising the LOC, FFA, PPA). In those experiments the Encoder and Decoder were trained on the subset of voxels using our RGBD method. We then evaluated the reconstructed depth maps by  $n$ -way rank identification ( $n=5, 10, 50, 100, 500$ , or 1000, lower is better). For comparison, we also plot the results when using all Visual Cortex voxels. We find that our depth reconstruction performance is dominantly driven by the activations from LVC voxels. Using voxels from HVC alone significantly degrades our depth recovery performance.

**Voxel-specific Depth Sensitivity Index.** We studied whether voxels can be characterized by their tuning to depth versus RGB-image information type. To this end, we used our trained RGBD Encoder, and computed the predicted voxel activations when setting each one of the RGBD input channels to zero (one channel at a time). More formally, given a set of RGBD images,  $\{(s_i)\}$ , we denote by  $s_{ki}$  the resulting image when setting channel  $k$  in  $s_i$  to zero ( $k \in \{R, G, B, D\}$ ).  $F_i = \text{Enc}(s_i)$  denotes the encoded fMRI of the original RGBD image  $s_i$ ,  $F_{ki} = \text{Enc}(s_{ki})$  denotes the encoded fMRI after zeroing channel  $k$  in  $s_i$ . We define Voxel Depth Sensitivity Index (VDSI) at voxel  $v$  as:

$$\text{VDSI}(v) = \frac{\mathbb{E}_i (|F_i(v) - F_{D,i}(v)|)}{\mathbb{E}_c (\mathbb{E}_j (|F_i(v) - F_{c,i}(v)|))} ; \text{VDSI}(v) \in [0, \text{inf}) . \quad (5)$$

where  $c$  is a color channel. Voxels with  $\text{VDSI} \approx 1$  have similar sensitivity to color and depth variations. Fig 5c shows the resulting VDSI values for all Visual Cortex voxels. We evaluated the VDSI on two datasets: (i) RGBD images from the external dataset, (ii) the fMRI test set (see Sec 4.1). The scatter plot (Kernel-Density-Estimate plot) in Fig 5c shows a strong agreement of the index across these two datasets (0.92 Pearson’s correlation). Similar agreement was also found with respect to the train and validation sets from the fMRI dataset. This consistency possibly suggests the reliability of our VDSI measure. Note, however, that the vast majority of voxels have VDSI value well below 1. Exploring this further and validating the depth-sensitivity of individual voxels is part of our future work.

## Conclusion

The proposed method is the first to reconstruct dense 3D depth information from brain activity. Our approach is capable of reconstructing depth-based information (*Depth-only* or *RGBD*) directly from fMRI recordings. We compensate for the lack in available fMRI training data by adding self-supervision on a very large collection of natural images *without fMRI*, along with their depth maps. We show that predicting the depth map *directly from fMRI* outperforms its indirect recovery from a reconstructed image. We further present a Depth-based Perceptual Similarity metric, which employs learned perceptual depth-based features. Lastly, we attempt to characterize the degree of depth-sensitivity of brain-voxels via a proposed depth-sensitivity measure. Exploring the validity of these depth-sensitivity predictions is part of our future work.

## Acknowledgments

This project has received funding from the European Research Council (ERC) under the European Union's Horizon 2020 research and innovation programme (grant agreement No 788535).

## References

- [1] Y. Kamitani and F. Tong, "Decoding the visual and subjective contents of the human brain," *Nature Neuroscience*, vol. 8, pp. 679–685, 5 2005.
- [2] J.-D. Haynes and G. Rees, "Decoding mental states from brain activity in humans," *Nature Reviews Neuroscience*, vol. 7, pp. 523–534, 7 2006.
- [3] K. N. Kay and J. L. Gallant, "I can see what you see," 3 2009.
- [4] T. Naselaris, R. J. Prenger, K. N. Kay, M. Oliver, and J. L. Gallant, "Bayesian Reconstruction of Natural Images from Human Brain Activity," *Neuron*, vol. 63, pp. 902–915, 9 2009.
- [5] A. V. Iyer and J. Burge, "Depth variation and stereo processing tasks in natural scenes," *Journal of Vision*, vol. 18, pp. 4–4, 6 2018.
- [6] I. P. Howard, *Perceiving in Depth*, vol. 1. Oxford University Press, 5 2012.
- [7] A. E. Welchman, "The Human Brain in Depth: How We See in 3D," 10 2016.
- [8] M. Armendariz, H. Ban, A. E. Welchman, and W. Vanduffel, "Areal differences in depth cue integration between monkey and human," *PLoS Biology*, vol. 17, p. e2006405, 3 2019.
- [9] K. N. Kay, T. Naselaris, R. J. Prenger, and J. L. Gallant, "Identifying natural images from human brain activity," *Nature*, vol. 452, pp. 352–355, 3 2008.
- [10] S. Nishimoto, A. T. Vu, T. Naselaris, Y. Benjamini, B. Yu, and J. L. Gallant, "Reconstructing visual experiences from brain activity evoked by natural movies.," *Current biology : CB*, vol. 21, pp. 1641–6, 10 2011.
- [11] H. Wen, J. Shi, Y. Zhang, K.-H. Lu, J. Cao, and Z. Liu, "Neural Encoding and Decoding with Deep Learning for Dynamic Natural Vision," *Cerebral Cortex*, vol. 28, pp. 4136–4160, 12 2018.
- [12] U. Guclu, M. A. J. van Gerven, U. Güçlü, and M. A. J. van Gerven, "Deep Neural Networks Reveal a Gradient in the Complexity of Neural Representations across the Ventral Stream," *Journal of Neuroscience*, vol. 35, pp. 10005–10014, 7 2015.
- [13] G. Shen, T. Horikawa, K. Majima, and Y. Kamitani, "Deep image reconstruction from human brain activity," *PLOS Computational Biology*, vol. 15, p. e1006633, 1 2019.
- [14] C. Zhang, K. Qiao, L. Wang, L. Tong, Y. Zeng, and B. Yan, "Constraint-Free Natural Image Reconstruction From fMRI Signals Based on Convolutional Neural Network," *Frontiers in Human Neuroscience*, vol. 12, p. 242, 6 2018.
- [15] K. Han, H. Wen, J. Shi, K.-H. Lu, Y. Zhang, D. Fu, and Z. Liu, "Variational autoencoder: An unsupervised model for encoding and decoding fMRI activity in visual cortex," *NeuroImage*, vol. 198, pp. 125–136, 9 2019.
- [16] Z. Ren, J. Li, X. Xue, X. Li, F. Yang, Z. Jiao, and X. Gao, "Reconstructing seen image from brain activity by visually-guided cognitive representation and adversarial learning," *NeuroImage*, vol. 228, p. 117602, 3 2021.
- [17] M. Mozafari, L. Reddy, and R. Vanrullen, "Reconstructing Natural Scenes from fMRI Patterns using BigBiGAN," tech. rep.
- [18] K. Qiao, J. Chen, L. Wang, C. Zhang, L. Tong, and B. Yan, "BigGAN-based Bayesian Reconstruction of Natural Images from Human Brain Activity," *Neuroscience*, vol. 444, pp. 92–105, 7 2020.
- [19] G. Shen, K. Dwivedi, K. Majima, T. Horikawa, and Y. Kamitani, "End-to-end deep image reconstruction from human brain activity," *Frontiers in Computational Neuroscience*, vol. 13, p. 21, 4 2019.
- [20] G. St-Yves and T. Naselaris, "Generative Adversarial Networks Conditioned on Brain Activity Reconstruct Seen Images," in *Proceedings - 2018 IEEE International Conference on Systems, Man, and Cybernetics, SMC 2018*, pp. 1054–1061, Institute of Electrical and Electronics Engineers Inc., 1 2019.

- [21] K. Seeliger, U. Güçlü, L. Ambrogioni, Y. Güçlütürk, and M. A. van Gerven, “Generative adversarial networks for reconstructing natural images from brain activity,” *NeuroImage*, vol. 181, pp. 775–785, 2018.
- [22] Y. Lin, J. Li, H. Wang, and S. Jiao, “DCNN-GAN: Reconstructing Realistic Image from fMRI,” tech. rep., 2019.
- [23] G. Gaziv, R. Belyi, N. Granot, A. Hoogi, F. Strappini, T. Golan, and M. Irani, “Self-Supervised Natural Image Reconstruction and Rich Semantic Classification from Brain Activity,” *bioRxiv*, p. 2020.09.06.284794, 9 2020.
- [24] R. Belyi, G. Gaziv, A. Hoogi, F. Strappini, T. Golan, and M. Irani, “From voxels to pixels and back: Self-supervision in natural-image reconstruction from fMRI,” in *Advances in Neural Information Processing Systems*, 2019.
- [25] K. Lasinger, R. Ranftl, K. Schindler, and V. Koltun, “Towards robust monocular depth estimation: Mixing datasets for zero-shot cross-dataset transfer,” 7 2019.
- [26] T. Horikawa and Y. Kamitani, “Generic decoding of seen and imagined objects using hierarchical visual features,” *Nature Communications*, vol. 8, p. 15037, 10 2015.
- [27] J. Deng, W. Dong, R. Socher, L.-J. Li, Kai Li, and Li Fei-Fei, “ImageNet: A large-scale hierarchical image database,” in *2009 IEEE Conference on Computer Vision and Pattern Recognition*, pp. 248–255, IEEE, 6 2009.
- [28] R. Zhang, P. Isola, A. A. Efros, E. Shechtman, and O. Wang, “The Unreasonable Effectiveness of Deep Features as a Perceptual Metric,” in *IEEE/CVF Conference on Computer Vision and Pattern Recognition (CVPR)*, 2018.